

Optimizing the multiphoton absorption properties of maximally path-entangled number states

William N. Plick, Christoph F. Wildfeuer, Petr M. Anisimov, and Jonathan P. Dowling
*Hearne Institute for Theoretical Physics, Department of Physics and Astronomy, Louisiana State University,
 Baton Rouge, Louisiana 70803, USA*

(Received 20 August 2009; published 9 December 2009)

In this paper we examine the N -photon absorption properties of maximally path-entangled number states ($N00N$ states). We consider two cases. The first involves the N -photon absorption properties of the ideal $N00N$ state, one that does not include spectral information. We study how the N -photon absorption probability of this state scales with N , confirming results presented by others in a previous paper by a different method. We compare this to the absorption probability of various other states. The second case is that of two-photon absorption for an $N=2$ $N00N$ state generated from a type-II spontaneous down-conversion event. In this situation we find that the absorption probability is both better than analogous coherent light (due to frequency entanglement) and highly dependent on the optical setup. We show that the poor production rates of quantum states of light may be partially mitigated by adjusting the spectral parameters to improve their two-photon absorption rates. This work has application to quantum imaging, particularly quantum lithography, where the N -photon absorbing process in the lithographic resist must be optimized for practical applications.

DOI: [10.1103/PhysRevA.80.063825](https://doi.org/10.1103/PhysRevA.80.063825)

PACS number(s): 42.50.St, 42.50.Hz, 85.40.Hp, 42.50.Dv

I. INTRODUCTION

We investigate the multiphoton absorption probabilities of maximally path-entangled number states—also called $N00N$ states, after the way the state vector is written: $|N::0\rangle \equiv (|N,0\rangle + |0,N\rangle)/\sqrt{2}$. The two positions in each state vector represent two spatial modes in an optical interferometer. So, for example, for modes 1 and 2 we abbreviate $|x\rangle_1|y\rangle_2$ as $|x,y\rangle$. These states are of interest due to the fact that they greatly improve the resolution and sensitivity of interferometry for metrology. Also, it has been shown that they would improve the resolution with which lithographic features may be written. We show that (monochromatic) $N00N$ state absorption fares poorly as N increases, reinforcing through separate means a more sophisticated model presented in [1]. Thus, when considering possible applications of these states, such as to quantum lithography [2,3] or metrology [4,5], we need to keep an eye toward maximizing these absorption rates by varying their spectral parameters. We do this knowing that it has been found that squeezed light can exhibit novel two-photon absorption properties, such as linear growth of absorption rate with intensity and decreasing absorption, for increasing field [6–8].

We consider in detail the case of a $|2::0\rangle$ state used in a quantum lithography or quantum metrology setup. We include spectral information and derive a general expression for the two-photon absorption probability. Then we numerically maximize the probability function and find the setup which maximizes the two-photon absorption. The absorption probability can be improved by several orders of magnitude by carefully adjusting the filter bandwidths, pump pulse length, and the length of the crystal. The absorption probability of $|2::0\rangle$ is shown to be much better than analogous coherent light. Though the $|2::0\rangle$ state would not be a desirable source for quantum lithography, our work shows that the absorption enhancement that the spectral properties of entangled light sources provide can compensate for their poor production rates. We go beyond most previous studies in that

we obtain the two-photon absorption probability directly instead of only considering the second-order correlation function.

In Sec. II we compare the absorption properties of ideal $N00N$ states to other states of light. In Sec. III we calculate the biphoton amplitude in the general case and then examine the absorption properties of this type of light in two regimes: the pulse-pumped and the continuous-wave-pumped. Some of the more lengthy calculations are left to the appendixes.

II. ABSORPTION PROPERTIES OF IDEAL $N00N$ STATES

Initially one may consider the ideal $N00N$ state: $|N::0\rangle$ [2]. This state contains no spectral information. It is an abstraction which can only exist in an optical cavity. Nonetheless, it will provide some insight into how the absorption properties of $N00N$ states compare to other sources.

Agarwal studied how multiphoton absorption rates are influenced by the specific properties of the incident light [9]. He found that the equation of motion for the field can be written as

$$\frac{\partial \langle \hat{a}^\dagger \hat{a} \rangle}{\partial t} = -2n\lambda^{(n)} \langle \hat{a}^\dagger \hat{a}^n \rangle.$$

Here, $\lambda^{(n)}$ is the absorption coefficient for the n -photon absorption process and contains information about the medium that is acting as the absorber, which is assumed to be much smaller spatially than the field (alternatively the field may be regarded as being spatially mode pure). Classically n -photon absorption is proportional to n th order intensity. Since we are comparing light sources of like intensities we make the substitution

$$\langle \hat{a}^\dagger \hat{a}^n \rangle = r_n \langle \hat{a}^\dagger \hat{a} \rangle^n,$$

where r_n represents the degree to which the quantum statistical characteristics of the light affect the n -photon absorp-

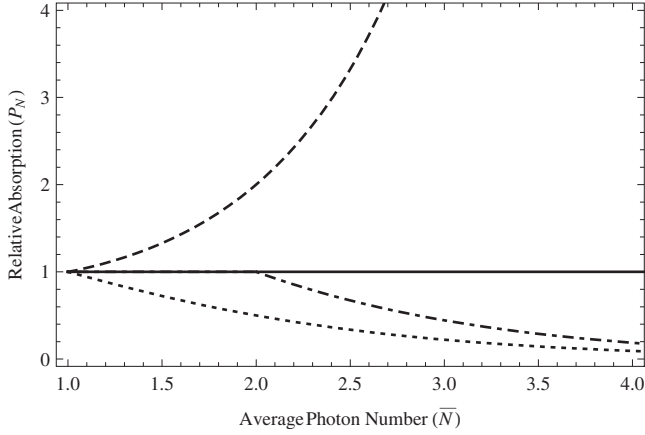


FIG. 1. Multiphoton absorption rate of various sources as a function of the average number of photons in the field (N th order absorption vs \bar{N} average photons). All rates normalized relative to coherent states (solid line). The dashed line is a thermal state. The dotted line is a Fock (number) state and the dot-dashed line is a $N00N$ state.

tion. Now the rate of change of the field due to multiphoton absorption is equivalent to r_n and a factor of several constants. Collecting these constants into one factor κ and renaming r_n as the relative absorption rate R_n we arrive at

$$R_n = \kappa \frac{\langle \hat{a}^{\dagger n} \hat{a}^n \rangle}{\langle \hat{a}^{\dagger} \hat{a} \rangle^n},$$

where κ is set to 1 in the interest of simplicity. We can use this information to produce a graph to see how the multiphoton absorption rate of $N00N$ states scale with N , when compared to quantum states that are not path entangled such as thermal, number, and coherent.

Thermal states are described by the following density matrix:

$$\hat{\rho}_{\text{thermal}} = \frac{1}{Z} \sum_{j=0}^{\infty} e^{-E_j/kT} |j\rangle\langle j|,$$

$$Z = \frac{e^{-\hbar\omega/2kT}}{1 - e^{-\hbar\omega/kT}}, \quad E_j = \hbar\omega \left(j + \frac{1}{2} \right).$$

Obtaining the matrices for number, coherent, and $N00N$ states is straightforward. For a two-mode state the annihilation operator is given as $\hat{a} = 1/\sqrt{2}(\hat{a}_1 + \hat{a}_2)$ where 1 and 2 label the two paths the photon may take [2].

See Fig. 1. Thermal states clearly have the greatest rates of multiphoton absorption. This can be attributed to the fact that thermal states exhibit bunching. That is, that photons from thermal radiation tend to be tightly correlated in time. Fock (number) states fare the worst. This feature of Fock states is connected to the fact that number states represent standing waves where the locations of the individual photons are evenly spaced out (or antibunched) in space and time with no definable phase. The multiphoton absorption properties of coherent states stay constant with respect to photon number. Since photons in coherent states are randomly dis-

persed in space and time the chance of two or more photons being correlated is simply proportional to the intensity (average photon number). Since we are considering how n -photon absorption scales against average photon number, the graph is flat, providing a convenient measuring stick to gauge other fields.

For $N00N$ states the multiphoton absorption behaves as

$$R_N = 1 \quad \text{for } N = 1,$$

$$= 2 \frac{N!}{N^N} \quad \text{for } N \geq 2.$$

$N00N$ states fare a factor of 2 better than Fock states, although absorption rates are still far from optimal. The reason $N00N$ states have this factor of 2 is due to the path entanglement. Mathematically this 2 comes from the normalization constant that path entanglement requires.

These results seem to reinforce the findings of Tsang in Ref. [1]: generally the absorption properties of $N00N$ states are poor. It should be re-emphasized that these states, containing no spectral or temporal information, are idealizations. Figure 1 can only be seen as providing a rough idea of how absorption scales.

Quantum lithography or metrology will only be useful if the detector or material needs to be exposed to the field for a reasonable period of time. The above ideal-field results seem to make this unlikely. However, they show only that the quantum-mechanical properties (i.e., the bare state vector) of $N00N$ states lead to poor absorption rates. They say nothing about how the spectral properties of realistic $N00N$ state pulses affect the multiphoton absorption probability. We thus examine in detail a specific well known case: the $|2:0\rangle$ state. Though this state is not practical for metrology or lithography its optimization would provide a proof of principle that the absorption properties of higher N states could be improved in a similar manner.

III. ABSORPTION PROPERTIES OF REALISTIC $|2:0\rangle$ STATES

It is possible to write realistic states, which include the spectral information of the light of interest. Furthermore, after these states are used to obtain absorption rates, the arrangement of optical elements which optimizes absorption can be found.

Going back to 1977 it has been shown that reducing the time interval between photons sharply increases two photon absorption probabilities [10]. Several works have examined how biphotons produced by parametric down-conversion or electromagnetically induced transparency may be compressed or otherwise modified so that they exhibit tighter correlations [11–16]. There is an excellent paper by Dayan which studies the properties of a semistationary undepleted beam of squeezed light produced by a spectrally narrow pump [17]. Also worthy of particular note is a paper by O’Donnell and U’Ren which demonstrates experimentally the ultrafast nonclassical correlation between entangled photons [18].

We consider the case of a $|2:0\rangle$ state used in a quantum lithography [2,3] or remote quantum metrology [4,5] setup.

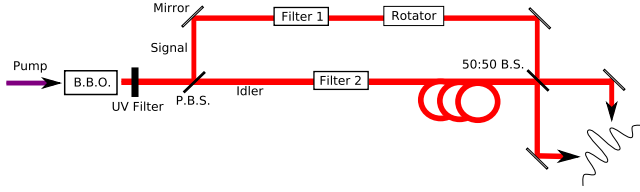


FIG. 2. (Color online) The basic setup. A nonlinear crystal (BBO in this case) creates a degenerate pair of photons. Each photon is subjected to a filter. A polarization rotator ensures that the two photons are indistinguishable. A beam splitter creates a $|2:0\rangle$ state that results in an interference pattern.

The $|2:0\rangle$ state we investigate is produced by collinear type-II degenerate down-conversion and a beam splitter (see Fig. 2). This setup is very simple, but by tuning these few basic optical elements we can see a large improvement in two-photon absorption rates, without recourse to exotic techniques. We make no assumptions about stationarity or about the relative sizes of the field bandwidths (apart from one very broadly applicable assumption—that the field’s bandwidth is narrower than the atomic transition frequencies; this will be discussed further in Appendix B).

A. Type-II biphoton

The output state of the crystal during type-II down-conversion is described by [19]

$$|\Psi\rangle = C \sum_{kk'} \int_0^\infty d\omega_p \int_0^L dz e^{-\mathcal{D}(\omega_p - \Omega_p)^2 / \sigma_p^2} e^{iz\Delta_{kk'}} \times \delta(\omega_{ok} + \omega_{ek'} - \omega_p) \hat{a}_{ok}^\dagger \hat{b}_{ek'}^\dagger |0\rangle_o |0\rangle_e \quad (1)$$

for a collinear pump. The sum extends over all possible wave-vector modes. A polarizing beam splitter separates the ordinary and extraordinary beams into different spatial modes. The operators \hat{a} and \hat{b} represent these modes. $\Delta_{kk'}$ is the phase mismatch defined as $k_p - k - k'$; ω_p is the frequency of the pump laser and the z integral extends over the length of the crystal. Ω_p and σ_p are the central frequency and the spectral full width at half maximum (FWHM) of the pump, respectively. e and o label the extraordinary and ordinary beams. The factor \mathcal{D} is defined as $4 \ln(2)$. We are assuming the pump laser is Fourier-transform limited.

This state corresponds to squeezing just above threshold such that mainly $|0,0\rangle$ and $|1,1\rangle$ are produced. The $|0,0\rangle$ term is then dropped because it cannot affect the two-photon absorption process.

Since the two beams are distinguishable after the polarizing beam splitter, one of the beams must be subject to a polarization rotator in order for it to be made indistinguishable from the other. The beams must be indistinguishable so that the $|1,1\rangle$ states interfere destructively and produce $|2:0\rangle$ [20].

To study the two-photon absorption probability of this state we utilize the well confirmed [21,22] Eqs. (2.15) and (2.16) from Mollow [23],

$$P_2 = \iint d\omega' d\omega g^*(\omega') S^{(2)}(\omega_f - \omega', \omega'; \omega_f - \omega, \omega) g(\omega), \quad (2)$$

where $g(\omega)$ is the atomic response function, ω_f is the frequency of the final state, and $S^{(2)}$ is the spectral correlation function (the Fourier transform of the temporal correlation function), which in our case is

$$S^{(2)}(\omega'_1, \omega'_2; \omega_1, \omega_2) = \mathcal{Z}(\omega'_1, \omega'_2)^* \mathcal{Z}(\omega_1, \omega_2), \quad (3)$$

where

$$\mathcal{Z}(\omega_1, \omega_2) \equiv \iint dt_1^d dt_2^d e^{i\omega_1 t_1^d} e^{i\omega_2 t_2^d} A(t_1^d, t_2^d).$$

Here, ω'_1 and ω'_2 represent the negative-frequency components of the field associated with $t_1^{d'}$ and $t_2^{d'}$. The factors ω_1 and ω_2 represent the positive-frequency components of the field associated with t_1^d and t_2^d . The above equation does not include the effects of natural linewidth, which will be discussed later. We should note that other equations, also derived by Mollow [23], assume that the field is stationary, something which is not true in general for our calculation here. A is the biphoton amplitude defined below.

We start with the two-photon correlation function [24]

$$G^{(2)} = \langle \Psi | \hat{E}^{(-)}(t_1^{d'}) \hat{E}^{(-)}(t_2^{d'}) \hat{E}^{(+)}(t_1^d) \hat{E}^{(+)}(t_2^d) | \Psi \rangle. \quad (4)$$

The primed and unprimed time variables represent the possibility of the biphoton traveling via two different paths of different lengths, as is the case in an interferometric setup, and d labels the times as being detection times. $\hat{E}^{(+)}(t)$ is the positive-frequency electric-field operator defined by

$$\hat{E}^{(+)}(t_j^d) = i \sum_{s,j,k_j} \left(\frac{\hbar \omega_{k_j}}{2\epsilon_0 V} \right)^{1/2} e^{-\mathcal{D}(\omega_{k_j} - \Omega_f)^2 / \sigma_f^2} e^{-i\omega_{k_j} t_j^d} \hat{a}_{s,j,k_j}(0), \quad (5)$$

where the approximation $e^{\pm i\mathbf{k}\cdot\mathbf{r}} \approx 1$ has been made and s denotes either horizontal or vertical polarization. The time $t^d = 0$ is defined as the time the photon is created. Note that $\hat{E}^{(+)\dagger} = \hat{E}^{(-)}$. Also, Ω_f and σ_f are the central frequency and the FWHM of the filter in a specific arm, respectively.

Now, by inserting a complete set of number states in the correlation function, and observing that all but the $|0\rangle\langle 0|$ term will cancel, we can rewrite Eq. (4) as

$$G^{(2)} = \langle \Psi | \hat{E}^{(-)}(t_1^{d'}) \hat{E}^{(-)}(t_2^{d'}) | 0\rangle\langle 0 | \hat{E}^{(+)}(t_1^d) \hat{E}^{(+)}(t_2^d) | \Psi \rangle \\ \equiv A(t_1^{d'}, t_2^{d'})^* A(t_1^d, t_2^d).$$

The above equation defines the biphoton amplitude $A(t_1^d, t_2^d)$. The expressions for A for SPDC were first calculated by Keller and Rubin in Ref. [25] and elaborated upon in Refs. [26–28]. We follow their calculations somewhat closely. For more details see Appendix A. The result is $A(t_1^d, t_2^d) = \mathcal{A}(t_1^d, t_2^d) + \mathcal{A}(t_2^d, t_1^d)$, where the script \mathcal{A} represents the biphoton amplitude for down-conversion followed by a polarizing beam splitter. The italic A is the biphoton amplitude for our setup. The result of our calculation for \mathcal{A} is

$$\begin{aligned} \mathcal{A}(t_1^d, t_2^d) = & e^{-i(\Omega_e t_2^d + \Omega_o t_1^d)} e^{-t_1^d O_U \sigma_o + t_2^d E_U \sigma_e} \sqrt{4\mathcal{D}U^2} \\ & \times \frac{U_e U_o U_p \sigma_e \sigma_o \sigma_p}{U\sqrt{\mathcal{D}}} [\text{erf}(T) - \text{erf}(T+l)], \end{aligned} \quad (6)$$

where

$$\begin{aligned} T = & \frac{(t_1^d - t_2^d) P_U \sigma_e \sigma_o + t_1^d E_U \sigma_o \sigma_p - t_2^d O_U \sigma_e \sigma_p}{2U\sqrt{\mathcal{D}(\sigma_e^2 + \sigma_o^2 + \sigma_p^2)}}, \\ l = & \frac{LU}{2U_e U_o U_p \sqrt{\mathcal{D}(\sigma_e^2 + \sigma_o^2 + \sigma_p^2)}}, \end{aligned}$$

and

$$\begin{aligned} P_U = & U_p(U_e - U_o)\sigma_e\sigma_o, \quad E_U = U_e(U_p - U_o)\sigma_p\sigma_o \\ O_U = & U_o(U_e - U_p)\sigma_e\sigma_p, \quad U^2 = P_U^2 + E_U^2 + O_U^2. \end{aligned}$$

The error function is commonly defined as

$$\text{erf}(x) = \frac{2}{\sqrt{\pi}} \int_0^x dy e^{-y^2}.$$

The terms U_e , U_o , and U_p represent the group velocities of the extraordinary, ordinary, and pump beams, respectively. The factors σ_e and σ_o are the bandwidths of the filters in the arms of the interferometer. The term σ_p is the bandwidth of the pump. The factors Ω_e and Ω_o are the central frequencies of the extraordinary and ordinary beams. For now the normalization constant has been left off for the sake of simplicity as it will only affect the height of the amplitude, not its overall shape.

Hence, we give the general biphoton amplitude in its most general form. In order to evaluate this expression we must find the group velocities of the pump, ordinary, and extraordinary beams inside of the $\chi^{(2)}$ crystal. The index of refraction as a function of wavelength can be found using the Sellmeier equations. Below are the Sellmeier equations for β -barium borate (BBO) [29]

$$\begin{aligned} n_o(\lambda_o) = & \sqrt{2.7359 + \frac{0.01878}{\lambda_o^2 - 0.01822} - 0.0135\lambda_o^2}, \\ n_e(\lambda_e) = & \sqrt{2.3753 + \frac{0.01224}{\lambda_e^2 - 0.01667} - 0.01516\lambda_e^2}, \end{aligned}$$

where the wavelength is given in micrometers. In type-II down-conversion in BBO the pump beam experiences the same index of refraction as the extraordinary beam. It is also important to consider the angle the beams form with respect to the optic axis of the crystal. Since we are investigating the degenerate collinear case with planar phase matching the optic axis must be set to be 42.4° off the pump beam's direction of propagation for a 400 nm pump (the ordinary and extraordinary beams are collinear with the pump and selected with a pinhole downstream) [27]. For the pump and extraordinary beams we must use the effective index of refraction given by

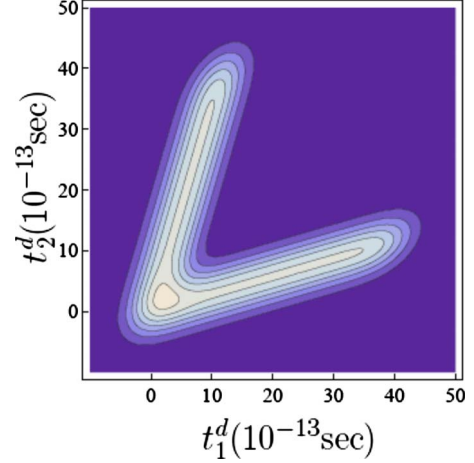


FIG. 3. (Color online) Contour plot of the absolute value of the biphoton amplitude for our setup $|A|$. $\sigma_e = \sigma_o = \sigma_p = 10^{13}$ Hz and $L = 1.5$ cm. t_1^d and t_2^d are in units of 10^{-13} sec.

$$n^{\text{eff}}(\lambda_e, \phi) = \left[\frac{\cos^2(\phi)}{n_o^2(\lambda)} + \frac{\sin^2(\phi)}{n_e^2(\lambda)} \right]^{-1/2},$$

where ϕ is the angle between the beam and the optic axis of the crystal. We can now calculate the group velocity

$$U_{e,o,p}(\lambda_{e,o,p}) = \left(\frac{n_{e,o,e}^{\text{eff}}(\lambda_{e,o,p})}{c} - \frac{\lambda_{e,o,p}}{c} \frac{\partial n_{e,o,e}^{\text{eff}}(\lambda_{e,o,p})}{\partial \lambda_{e,o,p}} \right)^{-1}$$

and $n_o^{\text{eff}} = n_o$. We then find for the degenerate case ($\Omega_o = \Omega_e$) for $\lambda_p = 400$ nm that $U_o(\Omega_o) = 1.781 \times 10^8$ m/s, $U_p(\Omega_p) = 1.756 \times 10^8$ m/s, and $U_e(\Omega_e) = 1.845 \times 10^8$ m/s.

Figure 3 contains a contour plot of the absolute value of the biphoton amplitude for our setup (A). This graph displays an interesting splitting which is symmetric about a line given by $t_1^d - t_2^d = 0$. Each point on this line represents a different average arrival time of the biphoton $(t_1^d + t_2^d)/2$, a line drawn perpendicular to this line of symmetry represents another axis. That axis defines an entanglement time (the temporal distance between the two photons) as $t_1^d - t_2^d$. The symmetric splitting represents the fact that two photons generated far away from the exit surface of the crystal will drift apart in time. Thus, as the average arrival time increases (a delay being indicative of more time spent in the crystal) the photons drift apart. The symmetry is a result of the interferometer scrambling the information corresponding to which photon took which path. So for a set average arrival time there is an equal probability that the e photon will arrive first or that the o one will.

We can check Eq. (6) by taking limits and comparing to known formulas. Taking the limit of the biphoton amplitude as σ_o and σ_e go to infinity (the case of no filtering) and keeping in mind that one of the definitions of the Heaviside step function is

$$H(x) = \lim_{k \rightarrow \infty} \frac{1}{2} [1 + \text{erf}(kx)], \quad (7)$$

we are left with

$$\mathcal{A}(t_1^d, t_2^d) = e^{-\sigma_p^2 t} \left[2H\left(A - \frac{B}{2}\right) - 2H\left(A + \frac{B}{2}\right) \right],$$

where

$$A = \frac{(t_1^d - t_2^d)U_e U_o + \frac{1}{2}L(U_e - U_o)}{2U_e U_o \sqrt{\mathcal{D}}},$$

$$B = \frac{L(U_e - U_o)}{2U_e U_o \sqrt{\mathcal{D}}},$$

$$J = \frac{[t_1^d U_o (U_e - U_p) + t_2^d U_e (U_p - U_o)]^2}{\sqrt{\mathcal{D}}(U_e - U_o)^2 U_p^2}.$$

Utilizing the identity

$$\text{Rect}\left(\frac{x}{\tau}\right) = H\left(x + \frac{\tau}{2}\right) - H\left(x - \frac{\tau}{2}\right),$$

where

$$\text{Rect}(x) = \begin{cases} 0 & \text{if } |x| > 0.5, \\ \frac{1}{2} & \text{if } |x| = 0.5, \\ 1 & \text{if } |x| < 0.5, \end{cases}$$

we obtain the expression

$$\mathcal{A}(t_1^d, t_2^d) = -2e^{-\sigma_p^2 J} \text{Rect}\left(\frac{A}{B}\right),$$

which is equivalent to the expression given by Kim *et al.* in Ref. [27].

Equation (2) given together with Eq. (A4) gives all the necessary information for calculating the two-photon absorption probability for $N00N$ states of $N=2$. Details of this calculation are given in Appendix B. The result is

$$\begin{aligned} \tilde{P}_2 &= \frac{C''}{L\sigma_p} \int_{-\infty}^{\infty} dv_f e^{-2\mathcal{D}v_f^2} [(u_e + u_2)^2 \sigma_e^2 U_2^2 + u_e^2 \sigma_e^2 U_2^2 + 1/\sigma_p^2] \\ &\times \frac{|\text{erf}(\mathcal{E}v_f) - \text{erf}(\mathcal{E}v_f - \mathcal{L})|^2}{\left[1 + 4\left(\frac{v_f}{\kappa_f}\right)^2\right]}, \end{aligned} \quad (8)$$

where

$$u_e = \frac{1}{U_p} - \frac{1}{U_e},$$

$$U_2 = \frac{1}{U_o} - \frac{1}{U_e},$$

$$\mathcal{E} = \frac{i\sqrt{\mathcal{D}}[U_2\sigma_o^2 + u_e(\sigma_e^2 + \sigma_o^2)]}{U_2\sigma_e\sigma_o\sqrt{\sigma_e^2 + \sigma_o^2}},$$

$$\mathcal{L} = \frac{LU_2\sigma_e\sigma_o}{2\sqrt{\mathcal{D}}(\sigma_e^2 + \sigma_o^2)},$$

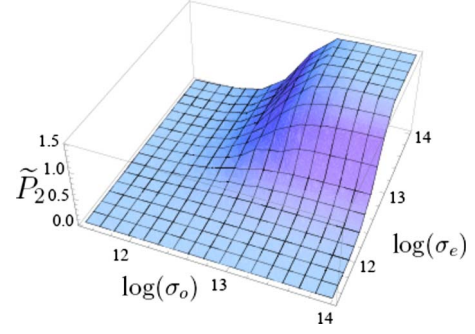


FIG. 4. (Color online) A plot of the scaled two-photon absorption probability for the realistic $|2: : 0\rangle$ state as a function of the logs (base 10) of the bandwidths of the filters in the arms of the interferometer (in hertz). $L=2.3$ mm, $\sigma_p=10^{12}$ Hz, and $\kappa_f=10^{14}$ Hz.

$$C'' = \frac{8}{U_2} (1 + \sqrt{\pi})^2 \sqrt{2\pi^7 \mathcal{D}}, \quad (9)$$

and κ_f is the FWHM of the final state. The atomic response function $g(\omega)$ can be moved outside the integral for the light sources we consider (see Appendix B for details). Unfortunately this integral is intractable analytically; we therefore perform the integration over v_f numerically.

B. Numerical calculation of type-II absorption rate

We wish to use Eqs. (2), (8), and (9) to calculate the relative absorption rate for type-II down-conversion. After this is done, we can use the information to maximize absorption by adjusting the available spectral parameters.

1. Pulse-pumped case

We start with the case of a pulsed pump. Since the two-photon absorption probability is a complicated quantity with five adjustable parameters (σ_e , σ_o , σ_p , L , and κ_f), we present several graphs to help elucidate the structure of this mathematical object. All of the graphs are scaled so that the maximal absorption probability—within the parameters we consider—is set to 1. Thus, $\tilde{P}_2=1$ does not represent an absorption probability of unity. The normalization is consistent across all the graphs so that they may be compared to one another on the same scale.

Figure 4 is a plot of the two-photon absorption as a function of the base-10 logarithms of the filter bandwidths. We see that a wider filter is preferable. This is because if the spectrum of the light is wide then the temporal distribution will be narrow, increasing the probability that the photons will arrive close together, triggering a two-photon absorption event.

Figure 5 is a plot of the two-photon absorption probability as a function of the logarithm base 10 of the bandwidth of the pump for several different atomic linewidths. Clearly a broader atomic linewidth will result in better absorption, as this will allow a greater range of frequency pairs to be absorbed. For the pump beam a smaller bandwidth is preferable. Once the bandwidth of the pump approaches that of the filters, or the linewidth of the atom, the absorption drop-off is

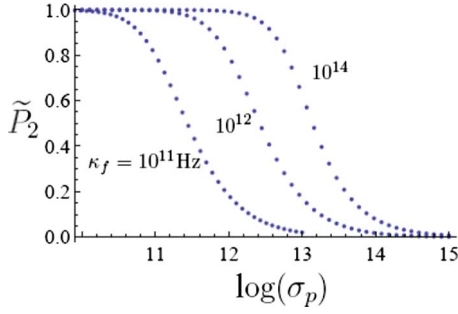


FIG. 5. (Color online) A plot of the scaled two-photon absorption probability for the realistic $|2:0\rangle$ state as a function of the log (base 10) of the bandwidth of the pump (in hertz) for three separate settings of the width of the final state of the absorber (in hertz). $L = 2.3$ mm and $\sigma_e = \sigma_o = 10^{13}$ Hz.

dramatic. Furthermore, a narrower pump bandwidth constrains the frequencies of the daughter photons increasing the probability that the sum of their energies will be resonant.

Figure 6 is a plot of the two-photon absorption probability of a $|2:0\rangle$ pulse as a function of crystal length for two separate cases. This is perhaps the most interesting of the representations of Eq. (8). The plot indicates the feature that for each setting of σ_o , σ_e , σ_p , and κ_f there is an optimal crystal length that maximizes the probability of two-photon absorption.

As light travels through the crystal the dispersive nature of the medium causes the two photons to drift apart in time. This effect results in a drop-off in absorption as length increases. Conversely, if the crystal length is very short, the spectrum of the light will be very broad, and the filters will strongly limit the amount of light that can reach the absorber. For broad filters, any deviation from the optimal length causes a dramatic drop-off in absorption. Information of this type would be useful when designing a two-photon quantum lithography experiment. A crystal cut to a specific length, for a given setup, would have the potential to enhance the two-photon absorption properties of the generated light.

By adjusting all the available parameters, significant improvement may be obtained. For example, take the case we have defined to be $\tilde{P}_2=1$: here we have chosen $\sigma_e = \sigma_o = 10^{13}$ Hz, $\sigma_p = 10^9$ Hz, $L = 2.3$ mm, and $\kappa_f = 10^{14}$ Hz. For the same absorber (κ_f the same), $\sigma_e = \sigma_o = 10^{11}$ Hz, σ_p

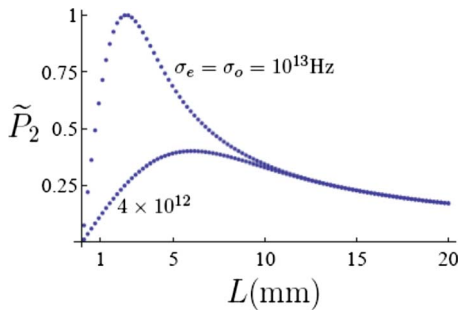


FIG. 6. (Color online) A plot of the scaled two-photon absorption probability for the realistic $|2:0\rangle$ state as a function of the length of the crystal for two different settings of the filters (in hertz). $\sigma_p = 10^{12}$ Hz and $\kappa_f = 10^{14}$ Hz.

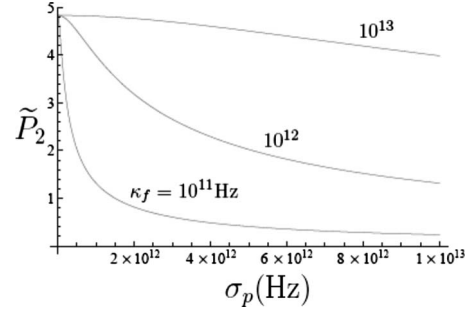


FIG. 7. A plot of the scaled two-photon absorption probability for the $|2:0\rangle$ state (in the limit of no filtering) as a function of the bandwidth of the pump. We indicate three separate settings of the width of the absorber. We also set $L = 1$ mm. The scaling is the same as on the other pulse-pumped plots.

$= 10^{13}$ Hz, and $L = 2$ cm, the absorption probability is $\tilde{P}_2 = 2.07 \times 10^{-5}$.

We may obtain completely analytical results for the case where there are no filters in the arms of the interferometer. Using Eq. (7), Eq. (8) becomes

$$\lim_{\sigma_e, \sigma_o \rightarrow \infty} \tilde{P}_2 = \frac{C'' \kappa_f e^{\mathcal{D} \kappa_f^2 / 8 \sigma_p^2}}{2L \sigma_p} K_0 \left(\frac{\mathcal{D} \kappa_f^2}{8 \sigma_p^2} \right), \quad (10)$$

so long as $L \neq 0$. The function K_n is the modified Bessel function of the second kind. Features of this function include a simple dependence on L and a modified σ_p dependence as shown in Fig. 7. Interestingly, for absorbers with very wide final states, the two-photon absorption probability becomes almost independent of the bandwidth of the pump.

In all cases, given a particular κ_f , a balance must be struck between the related quantities of temporal and spectral correlation. Tight temporal correlation increases the probability of absorption. However, this necessitates broad spectral distributions which have a lower probability of matching the correct energy for transition.

2. Comparison to coherent light

We can now tell how varying the spectral properties of $|2:0\rangle$ states will affect the absorption probability. However, we have discovered nothing about how $|2:0\rangle$ light's absorption properties compare to other, more familiar, states of light. We would like to say whether $|2:0\rangle$ has any benefits or disadvantages when compared to, for example, coherent light. Coherent light has the advantage of being relatively well understood (or at least very extensively studied). Thus, we shall attempt to find a state of coherent light which will serve as a fair comparison to $|2:0\rangle$, as produced in the fashion presented in this paper. We would like this fair state to have the same spectral profile as $|2:0\rangle$, but to lack the unique properties that the $N00N$ state possesses: momentum entanglement and a high degree of temporal correlation. For details on the derivation of this state see Appendix C. The result for the two-photon absorption probability is

$$\begin{aligned} \tilde{P}_2^\alpha &= \pi I^2 \operatorname{erf}\left(\frac{Lu_o\sigma_p}{\sqrt{2D}}\right)^{-2} \int_{-\infty}^{\infty} d\nu_f e^{-D(u_o-u_e)^2\nu_f^2/u_o^2\sigma_p^2} \\ &\times \frac{|\operatorname{erf}(\mathcal{E}_\alpha\nu_f) - \operatorname{erf}(\mathcal{E}_\alpha\nu_f + \mathcal{L}_\alpha)|^2}{\left[1 + 4\left(\frac{\nu_f}{\kappa_f}\right)^2\right]}, \end{aligned} \quad (11)$$

where

$$\begin{aligned} \mathcal{E}_\alpha &= \frac{i\sqrt{D}(u_o-u_e)}{\sqrt{2}u_o\sigma_p}, \\ \mathcal{L}_\alpha &= \frac{Lu_o\sigma_p}{\sqrt{2D}}, \end{aligned} \quad (12)$$

and $u_e = 1/U_p - 1/U_e$ and $u_o = 1/U_p - 1/U_o$. Here, I is the intensity of the light in each arm of the interferometer (i.e., $2I$ would be the total amount of light in the device).

This fair-comparison light can be thought of as a very spectrally broad coherent source incident on a magic “filter,” which imposes on it the same spectral profile as the $|2: :0\rangle$ state. Two spatial modes of this light are then used as the input into an interferometer without filters in the arms. The two-photon absorber is placed at the far end.

The error functions in the above coherent-state expression diverge much more rapidly than for the $|2: :0\rangle$ case. Thus, it is only possible to compute P_2^α for relatively narrow arguments of the integral over ν_f , so we must consider a non-maximal setup as a test case. So for $\sigma_p = 10^9$ Hz, $\kappa_f = 10^{10}$ Hz, and $L = 1$ cm we have

$$\tilde{P}_2^\alpha = 5.65 \times 10^{-6} \tilde{P}_2 I^2,$$

where \tilde{P}_2 has been calculated using Eq. (8).

If the intensities of the two kinds of light are set to be equal ($I=1$ in the above equation) then $|2: :0\rangle$ is absorbed with a much higher probability than coherent light. This is directly a result of the frequency entanglement. Maximal absorption probability occurs when the photon energies add, such that the total is the same as the center of the final level. For SPDC it is ensured that this condition will be closely met (exactly met in the case of a cw pump and a very thin crystal). However, for the coherent analog there is no such requirement; in fact the probability of two randomly chosen photons from the coherent pulses adding up to the resonance energy is miniscule. Even so, the above equation may be overly *optimistic* about the absorption properties of coherent light. Recall that we were forced to consider narrow-band fields to make the calculation numerically tractable. The effect that causes coherent light to have a poor two-photon absorption probability will be worsened when the bandwidth is broader; a regime in which the $|2: :0\rangle$ states’ absorption probability improves.

These positive results for the multiphoton absorption of entangled light are in seeming contradiction to the results of Sec. II, which shows that coherent states should fair better than $|N: :0\rangle$ states, where N -photon absorption is concerned. However, that treatment does not take into account the spectral properties of highly quantum-mechanical states of light,

which are likely to have high degrees of temporal correlation.

In a paper by Tsang [1], it was shown that the *spatial* properties of $N00N$ states cause them to have poor N -photon absorption rates. The relationship found in that paper is that $N00N$ states have absorption rates that are lower than a classical analog (in his case a monochromatic Fock state incident on a beam splitter) by a factor of $1/2^{N-1}$ due to spatial considerations independent of temporal correlations. He leaves open the question of whether time-domain effects can compensate for this effect. Given our above results it seems likely that the answer to this question is yes.

However, the advantage entangled light enjoys is offset by the fact that SPDC has an extremely small intensity. Even relatively high production efficiencies are only approximately one pair per 10^{12} incident photons (see, for example, Ref. [30]). Furthermore, it has been shown that correlated two-photon absorption (absorption from two photons of the same pair as opposed to absorption from two photons of different pairs) from entangled light dominates only when the intensity is small [31]. This makes it even more important to improve absorption rates.

It could also be pointed out that $|2: :0\rangle$ light is not a good candidate for lithography or metrology due to the fact that the pump light could just be used at double the frequency to achieve the same enhancement. This paper does not suggest, however, that it would be. Instead the purpose of our analysis is to take a simple case of the $|N: :0\rangle$ state ($N=2$) and show that the phenomenon of frequency entanglement prevalent in quantum-mechanical states of light, boosts multiphoton absorption to a degree which may counteract, or at least partially mitigate, small production rates. In this light our work may be viewed as a proof of principle. When $|N: :0\rangle$ states of large N become available it is highly likely that an analysis similar to the one presented in this section may be utilized to enhance the N -photon absorption rate. One might even conjecture—from the above discussion—that for higher N the temporal advantage of using entangled light may be more pronounced, since for classical light the problem of arranging for N photons to arrive at the same time is compounded as N increases.

3. Continuous-wave-pumped case

Let us now investigate the case of a continuous-wave pump. The expressions derived in the previous section only make sense when considering a biphoton *pulse*. They give the absorption probability of a biphoton of finite extent being absorbed as it passes an atom or other absorber. Note that since the pulses are Gaussian-like they are not strictly finite, but they are so closely temporally correlated that we may treat them as such. However the continuous-wave case is stationary. We must now speak of a two-photon absorption *rate*.

First we recalculate the biphoton amplitude. Take Eq. (A1), for a cw pump we set $\sigma_p = 0$ and $\omega_{k_o} + \omega_{k_e} = \Omega_p$. We can then rewrite this equation as

$$\begin{aligned} \mathcal{A}(t_1^d, t_2^d)_{\text{cw}} &= \sum_{k_o k_e} e^{-\mathcal{D}(\omega_{k_o} - \Omega_o)^2 / \sigma_o^2} e^{-i\omega_{k_o} t_1^d} e^{-\mathcal{D}(\omega_{k_e} - \Omega_e)^2 / \sigma_e^2} e^{-i\omega_{k_e} t_2^d} \\ &\quad \times \int_0^L dz e^{iz\Delta_{k_o k_e}} \delta(\omega_{k_o} + \omega_{k_e} - \Omega_p) \\ &= \frac{e^{-i(\Omega_o t_1^d + \Omega_e t_2^d)}}{U_e U_o} \int_{-\infty}^{\infty} d\nu \int_0^L dz e^{-\mathcal{D}(\nu/\sigma)^2} e^{-i\nu(t_2^d - t_1^d)} e^{iz\Delta_{k_o k_e}}, \end{aligned}$$

where

$$\sigma = \frac{\sigma_e \sigma_o}{\sqrt{\sigma_e^2 + \sigma_o^2}}.$$

In the second equality we have taken the continuous limit, changed variables from momentum to frequency, performed one of these integrals to eliminate the delta function, and then changed variables again to $|\nu_e| = |\nu_o| \equiv \nu$. We are able to do this due to conservation of energy for a cw pump: once the momentum of one photon is chosen the momentum of the other one is determined. Also the phase mismatch becomes

$$\Delta_{k_e k_o} = \nu \left(\frac{U_e - U_o}{U_e U_o} \right) \equiv u\nu.$$

We now write in analogy to Eq. (A4)

$$\begin{aligned} \mathcal{A}(t_1^d, t_2^d)_{\text{cw}} &= \frac{e^{-i(\Omega_o t_1^d + \Omega_e t_2^d)}}{U_e U_o} \int_0^L dz \hat{\mathcal{F}}(\nu \rightarrow [t_2^d - t_1^d]) Y(\nu), \\ Y(\nu) &= e^{-\mathcal{D}(\nu/\sigma)^2} e^{izuv}. \end{aligned}$$

The solution for A is easily found,

$$\begin{aligned} \mathcal{A}(t_1^d, t_2^d)_{\text{cw}} &= \frac{e^{-i(\Omega_o t_1^d + \Omega_e t_2^d)}}{U_e - U_o} \left[\operatorname{erf} \left(\sigma \frac{(t_1^d - t_2^d)}{2\sqrt{\mathcal{D}}} \right) \right. \\ &\quad \left. - \operatorname{erf} \left(\sigma \frac{(t_1^d - t_2^d) - Lu}{2\sqrt{\mathcal{D}}} \right) \right]. \end{aligned}$$

The absorption rate for stationary states is given by Eq. (3.17a) in Ref. [23],

$$w_2 = 2 \left| g \left(\frac{1}{2} \Omega_p \right) \right|^2 \int_{-\infty}^{\infty} dt e^{2i\Omega_p t - \kappa_f |t|} G^{(2)}(-t, -t; t, t),$$

where κ_f is the width of the final state of the absorber. We have for the second-order correlation function,

$$G^{(2)}(-t, -t; t, t) = \frac{2e^{-2i\Omega_p t}}{(U_e - U_o)^2} \left| \operatorname{erf} \left(\frac{Lu\sigma}{2\sqrt{\mathcal{D}}} \right) \right|^2,$$

and thus

$$w_2 = \frac{2 \left| g \left(\frac{1}{2} \Omega_p \right) \right|^2}{(U_e - U_o)^2} \left| \operatorname{erf} \left(\frac{Lu\sigma}{2\sqrt{\mathcal{D}}} \right) \right|^2 \int_{-\infty}^{\infty} dt e^{-\kappa_f |t|}.$$

The modulus squared of the error function is the only part that is dependent on the spectral properties of the field, so we

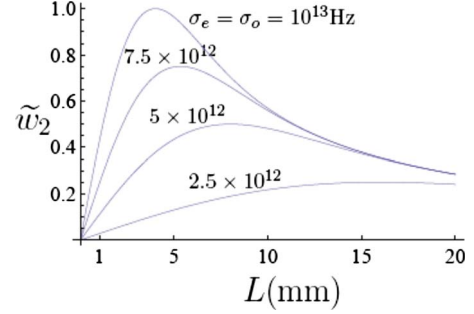


FIG. 8. (Color online) Plot of the two-photon absorption rate from a cw-pumped crystal, as a function of crystal length, for four separate settings of the filters (in hertz).

fold the overall constants into the atomic response function, which we will then ignore. We then obtain the relatively simple result

$$\tilde{w}_2 = \frac{1}{L} \left| \operatorname{erf} \left(\frac{Lu\sigma}{2\sqrt{\mathcal{D}}} \right) \right|^2, \quad (13)$$

where the factor of $1/L$ comes from the state normalization. Unlike for the general case, the cw expression is fully analytical. Figures 8 and 9 are plots of the absorption rate as a function of crystal length and filter bandwidths. The graphs have been normalized such that the greatest absorption rate for the range of parameters we consider is set to $\tilde{w}_2 = 1$.

So for a cw pump we have generally the same results as in the pulse-pumped case, with absorption improving as bandwidth increases. We also again observe that the graph of \tilde{w}_2 as a function of L displays peak values.

IV. CONCLUSION

First, we analyzed the multiphoton absorption probability of states of the form $|N: : 0\rangle$ in the ideal case (with no spectral information). We found that the absorption probability scales poorly with N when compared to coherent states, but well when compared to Fock states. Thus, we reinforced the original findings of [1] through less sophisticated means.

Second, we considered the case of a realistic $|2: : 0\rangle$ state produced by type-II spontaneous parametric down-conversion, a polarization rotator, and a beam splitter. We

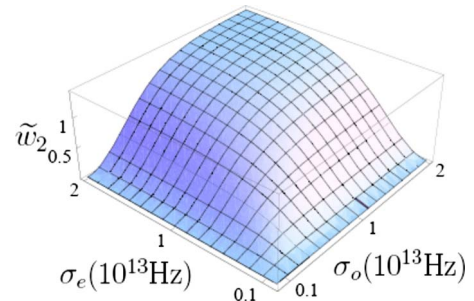


FIG. 9. (Color online) Plot of the two-photon absorption rate from a cw-pumped crystal as a function of the bandwidths of the filters in the ordinary and extraordinary arms. Here $L=6$ mm.

found that generally the two-photon absorption properties of this state are highly dependent on the specific optical setup used. Using numerical methods it is possible to analyze the absorption probability as a function of the realistic parameters of the experiment. We can then adjust the optical setup of our model including the length of the crystal, the bandwidths of the filters in the extraordinary and ordinary beams, and the pulse length of the pump. Running a maximization procedure over these variables it is possible to find the setup, which optimizes two-photon absorption. The difference between the optimal setup and a slight deviation may be dramatic.

This research constitutes a proof of principle of the idea that the poor production rates and detrimental spatial effects of highly quantum-mechanical states of light may be mitigated by improving the absorption rates through spectral means. Though we consider in detail only the $|2: : 0\rangle$ case, it is likely that once methods of developing $N00N$ states of higher N are developed, similar methods may be applied to improve their N photon absorption properties as well.

Also, in a broader sense, similar techniques may be applied to increase the multiphoton absorption properties of any desirable state of light. All that is required is the quantum-mechanical state vector.

ACKNOWLEDGMENTS

We would like to acknowledge the Army Research Office, the Boeing Corporation, The Foundational Questions Institute, the Intelligence Advanced Research Projects Activity, and the Northrup-Grumman Corporation for support. W.N.P. would also like to acknowledge the Louisiana Board of Regents for funding. Discussions with S. Vinjanampathy, S. Thanvanthri, and G. S. Agarwal were invaluable.

APPENDIX A: CALCULATION OF THE BIPHOTON AMPLITUDE

We start with a field at the detector given by Eq. (5). Using the standard 50:50 beam splitter transformation we write out the electric-field operator at the crystal

$$E^{(+)}(t^d) = \xi \sum_{k_1} (e^{-D(\omega_{k_1}^2/\sigma_o^2)} \hat{a}_{k_1} + i e^{-D(\omega_{k_1}^2/\sigma_e^2)} \hat{b}_{k_1}) \frac{e^{-i\omega_1 \tau}}{\sqrt{2}} \\ + \xi \sum_{k_2} (i e^{-D(\omega_{k_2}^2/\sigma_o^2)} \hat{a}_{k_2} + e^{-D(\omega_{k_2}^2/\sigma_e^2)} \hat{b}_{k_2}) \frac{e^{-i\omega_2 \tau}}{\sqrt{2}},$$

where constants have been subsumed into the overall factor of ξ . The polynomials ω_{k_j} have been ignored because they vary slowly when compared to the exponential terms. The operators \hat{a} and \hat{b} are the annihilation operators acting on the first and second modes. The two mode annihilation operators are used to signify that the amplitude is dependent on the fields in both spatial modes. $\tau = t^d - l/c$, where l is the distance between the crystal and the detector. We only consider

the case where the interferometer is path balanced. This implies we calculate the absorption properties of the central fringe. We assume that the absorption properties of the other fringes will behave similarly.

Now using the above and Eqs. (1) and (4) we can find an expression for the biphoton amplitude of our setup

$$A(t_1^d, t_2^d) = \mathcal{A}(t_1^d, t_2^d) + \mathcal{A}(t_2^d, t_1^d),$$

where \mathcal{A} is the biphoton amplitude for just the output of BBO and filters

$$\mathcal{A}(t_1^d, t_2^d) = iC\xi^2 \sum_{k_o k_e} e^{-D(\omega_{k_o} - \Omega_o)^2/\sigma_o^2} e^{-i\omega_{k_o} t_1^d} e^{-D(\omega_{k_e} - \Omega_e)^2/\sigma_e^2} \\ \times e^{-i\omega_{k_e} t_2^d} \int_0^L dz e^{-D(\omega_{k_o} + \omega_{k_e} - \Omega_p)^2/\sigma_p^2} e^{iz\Delta_{k_o k_e}}. \quad (\text{A1})$$

We have dropped the factor of $e^{-il/c}$ as it just introduces an overall phase. The central frequencies of the filters have been chosen to be the same as for the e and o rays.

Now, define the following variables:

$$\nu_o \equiv \omega_o - \Omega_o,$$

$$\nu_e \equiv \omega_e - \Omega_e,$$

$$\nu_p \equiv \omega_p - \Omega_p. \quad (\text{A2})$$

Due to the delta function in Eq. (1), $\Omega_o + \Omega_e = \Omega_p$ and $\nu_o + \nu_e = \nu_p$. Now, Taylor series expand the wave vector out to second order,

$$k(\nu_j) = k(\Omega_j) + \nu_j \left[\frac{dk(\nu_j)}{d\omega_j} \right]_{\omega_j = \Omega_j} = k(\Omega_j) + \frac{\nu_j}{U_j(\Omega_j)},$$

where $j=e, o, p$, and U is the group velocity and $U = d\omega/dk$. Taking into account that $k_p(\Omega_p) = k_e(\Omega_e) + k_o(\Omega_o)$ the phase mismatch can now be rewritten as

$$\Delta_{k_o k_e} = \frac{\nu_p}{U_p(\Omega_p)} - \frac{\nu_o}{U_o(\Omega_o)} - \frac{\nu_e}{U_e(\Omega_e)} \\ = \frac{\nu_o + \nu_e}{U_p(\Omega_p)} - \frac{\nu_o}{U_o(\Omega_o)} - \frac{\nu_e}{U_e(\Omega_e)}. \quad (\text{A3})$$

Taking the continuous limit of Eq. (A1) and utilizing Eqs. (A2) and (A3) we obtain

$$\mathcal{A}(t_1^d, t_2^d) = iC\xi^2 \int dk_o \int dk_e \int_0^L dz e^{-D(\nu_o/\sigma_o)^2} e^{-D(\nu_e/\sigma_e)^2} \\ \times e^{-i(\nu_e + \Omega_e)t_2^d} e^{-i(\nu_o + \Omega_o)t_1^d} e^{-D(\nu_o + \nu_e)^2/\sigma_p^2} e^{iz(u_e \nu_e + u_o \nu_o)},$$

where $u_e = 1/U_p - 1/U_e$ and $u_o = 1/U_p - 1/U_o$. Note that $dk = \frac{dk}{d\omega} d\omega = \frac{1}{U} d\omega = \frac{1}{U} d\nu$, so that up to a constant we may switch integration variables between momentum and frequency. (Actually the U 's are frequency dependent; however, they do

not vary significantly over the bandwidth of the field.) Here we diverge from Kim and Shih in that we integrate over ν_o and ν_e instead of $\nu_- \equiv \nu_o - \nu_e$ and ν_p and we do not take the filter bandwidths to be equivalent. Now

$$\begin{aligned} \mathcal{A}(t_1^d, t_2^d) &= \frac{iC\xi^2}{U_e U_o} e^{-i(\Omega_o t_1^d + \Omega_e t_2^d)} \int d\nu_o \int d\nu_e \int_0^L dz e^{-\mathcal{D}(\nu_o/\sigma_o)^2} \\ &\quad \times e^{-\mathcal{D}(\nu_e/\sigma_e)^2} e^{-i\nu_e t_2^d} e^{-i\nu_o t_1^d} e^{-\mathcal{D}(\nu_o + \nu_e)^2/\sigma_p^2} e^{iz(u_e \nu_e + u_o \nu_o)}. \end{aligned}$$

We have the unitary Fourier transform over ν_o , ν_e (up to a factor of $\sqrt{2\pi}$), and the integral over z given by

$$\begin{aligned} \mathcal{A}(t_1^d, t_2^d) &= \frac{2\pi i C \xi^2}{U_e U_o} e^{-i(\Omega_o t_1^d + \Omega_e t_2^d)} \int_0^L dz \hat{\mathcal{F}}(\nu_e \rightarrow t_2^d) \\ &\quad \times \hat{\mathcal{F}}(\nu_o \rightarrow t_1^d) \Upsilon(\nu_o, \nu_e, z), \end{aligned}$$

$$\Upsilon(\nu_o, \nu_e, z) = e^{-\mathcal{D}[(\nu_o + \nu_e)^2/\sigma_p^2 + (\nu_o/\sigma_o)^2 + (\nu_e/\sigma_e)^2]} e^{iz(u_e \nu_e + u_o \nu_o)}, \quad (\text{A4})$$

where we have defined the biphoton kernel $\Upsilon(\nu_o, \nu_e, z)$. In the interest of clarity the Fourier transforms have been written as operators

$$\hat{\mathcal{F}}(x \rightarrow y) \equiv \frac{1}{\sqrt{2\pi}} \int_{-\infty}^{\infty} dx e^{-ixy}.$$

Using MATHEMATICA™, we perform these operations in the above order. Note that another ordering will lead to the problem becoming intractable. The result is given by Eq. (6). For the sake of simplicity in most of our calculations we will take $\xi=1$.

State normalization

The state $|\Psi\rangle$ needs to be normalized. Take again Eq. (1) where the integral over ω_p has been performed,

$$|\Psi\rangle = C \sum_{k_e k_o} \int_0^L dz e^{-\mathcal{D}(\nu_e + \nu_o)^2/\sigma_p^2} e^{iz\Delta_{k_e k_o}} \hat{a}_e^\dagger \hat{a}_o^\dagger |0\rangle.$$

Now we take the inner product

$$\begin{aligned} \mathcal{Z}(\omega_o, \omega_e) &= 2\pi \hat{\mathcal{F}}(t_1^d \rightarrow \omega_o)^* \hat{\mathcal{F}}(t_2^d \rightarrow \omega_e)^* A(t_1^d, t_2^d) \\ &= 2\pi \hat{\mathcal{F}}(t_1^d \rightarrow \omega_o)^* \hat{\mathcal{F}}(t_2^d \rightarrow \omega_e)^* \mathcal{A}(t_1^d, t_2^d) + 2\pi \hat{\mathcal{F}}(t_1^d \rightarrow \omega_o)^* \hat{\mathcal{F}}(t_2^d \rightarrow \omega_e)^* \mathcal{A}(t_2^d, t_1^d) \\ &= C' \hat{\mathcal{F}}(t_1^d \rightarrow \omega_o)^* \hat{\mathcal{F}}(t_2^d \rightarrow \omega_e)^* e^{-i(\Omega_o t_1^d + \Omega_e t_2^d)} \int_0^L dz \hat{\mathcal{F}}(\nu_e \rightarrow t_2^d) \hat{\mathcal{F}}(\nu_o \rightarrow t_1^d) \Upsilon(\nu_o, \nu_e, z) \\ &\quad + C' \hat{\mathcal{F}}(t_1^d \rightarrow \omega_o)^* \hat{\mathcal{F}}(t_2^d \rightarrow \omega_e)^* e^{-i(\Omega_o t_2^d + \Omega_e t_1^d)} \int_0^L dz \hat{\mathcal{F}}(\nu_e \rightarrow t_1^d) \hat{\mathcal{F}}(\nu_o \rightarrow t_2^d) \Upsilon(\nu_o, \nu_e, z) \\ &= C' \int_0^L dz \hat{\mathcal{F}}(t_2^d \rightarrow \nu_e)^* \hat{\mathcal{F}}(\nu_e \rightarrow t_2^d) \hat{\mathcal{F}}(t_1^d \rightarrow \nu_o)^* \hat{\mathcal{F}}(\nu_o \rightarrow t_1^d) \Upsilon(\nu_o, \nu_e, z) \end{aligned}$$

$$\begin{aligned} \langle \Psi | \Psi \rangle &= \frac{4C^2}{U_e^2 U_o^2} \int_{-\infty}^{\infty} \int_{-\infty}^{\infty} d\nu_e d\nu_o e^{-2\mathcal{D}(\nu_e + \nu_o)^2/\sigma_p^2} \\ &\quad \times \frac{\sin^2\left(\frac{L}{2}[\nu_e u_e + \nu_o u_o]\right)}{[\nu_e u_e + \nu_o u_o]^2}, \end{aligned}$$

where we have taken the continuous limit and switched integration variables. It is required that $\langle \Psi | \Psi \rangle = 1$. We make another change of variables: $p = \nu_e + \nu_o$ and $q = \nu_e u_e + \nu_o u_o$, as long as $U_e \neq U_o$ this is a well defined one-to-one transformation with a Jacobian $J = U_e U_o / (U_e - U_o)$. This allows us to separate the integral. Thus,

$$\begin{aligned} &\frac{4C^2}{U_e U_o (U_e - U_o)} \int_{-\infty}^{\infty} dp e^{-2\mathcal{D}(p/\sigma_p)^2} \int_{-\infty}^{\infty} dq \frac{\sin^2\left(\frac{L}{2}q\right)}{q^2} \\ &= \frac{2C^2}{U_e U_o (U_e - U_o)} \frac{\pi^{3/2} L \sigma_p}{\sqrt{2\mathcal{D}}}. \end{aligned}$$

So

$$C = \left(\frac{\mathcal{D}}{2}\right)^{1/4} \frac{\sqrt{U_e U_o (U_e - U_o)}}{\pi^{3/4} \sqrt{L} \sigma_p}.$$

This factor is added onto Eq. (8). Using a similar procedure we obtain for the continuous-wave case

$$C_{\text{cw}} = \sqrt{\frac{U_e U_o (U_e - U_o)}{2\pi L}},$$

which we append to Eq. (13).

APPENDIX B: CALCULATION OF THE TWO-PHOTON ABSORPTION PROBABILITY FOR $N00N$ STATES

Noting that Eq. (3) represents a unitary transform back from time space into frequency space we may write the \mathcal{Z} function as

$$\mathcal{Z}(\omega_o, \omega_e) = 2\pi \hat{\mathcal{F}}(t_1^d \rightarrow \omega_o)^* \hat{\mathcal{F}}(t_2^d \rightarrow \omega_e)^* A(t_1^d, t_2^d).$$

Therefore,

$$\begin{aligned}
& + C' \int_0^L dz \hat{\mathcal{F}}(t_1^d \rightarrow \nu_o)^* \hat{\mathcal{F}}(\nu_e \rightarrow t_1^d) \hat{\mathcal{F}}(t_2^d \rightarrow \nu_e) \hat{\mathcal{F}}(\nu_o \rightarrow t_2^d) Y(\nu_o, \nu_e, z) \\
& = C' \int_0^L dz Y(\nu_o, \nu_e, z) + C' \int_0^L dz Y(\nu_e, \nu_o, z). \tag{B1}
\end{aligned}$$

In the second equality we have made a substitution using Eq. (A1). In the third equality Eq. (A4) was used. In the fourth equality the overall phases have combined with the Fourier-transform operators to change their output variables. So the Fourier transforms from the biphoton amplitude exactly cancel with the Fourier transforms from the definition of the spectral correlation function leaving a relatively simple result. Note that $Y(\nu_o, \nu_e, z) \neq Y(\nu_e, \nu_o, z)$ and

$$C' = 2\pi i (8\pi\mathcal{D})^{1/4} \sqrt{\frac{U_2}{L\sigma_p}},$$

where U_2 is defined in the main text. Returning to Eq. (2) we make the assumption that $g(\omega) \approx g(\frac{1}{2}\Omega_p)$. To see why, we need to investigate the definition of the atomic response function, Eq. (3.8) from Mollow [23],

$$g(\omega) = \mu \sum_j p_{fj} p_{j0} \frac{1}{\omega - \omega_j + \frac{1}{2}i\kappa_j},$$

where μ is a constant representative of the absorber, j labels the possible intermediate (virtual) levels, p_{j0} and p_{fj} are the momentum matrix elements of the electron making a transition between the initial and j th states, and the j th and final states, respectively. κ_j is the linewidth of the intermediate level. Each term in the series represents the two-photon absorption process proceeding via a different intermediate level transition. We assume that the central frequency of the field is one half the resonant frequency of the final state. Note that each term of g is highly peaked around the characteristic frequency of the level, which will be far detuned from the central frequency of the field. Unless the bandwidth of the field is on the order of the transition frequency, the value of the atomic response function will not change much as ω is varied over the bandwidth of the incident light. Therefore, our assumption is justified. Note that this is the *only* assumption we make about bandwidths in this paper. It is worth noting that there has been much work done toward engineering materials which have large two-photon cross sections [32,33], so as light sources are improving, so are absorbers.

So, using Eqs. (B1) and (2) we have

$$\begin{aligned}
P_2 = & \left| C' g\left(\frac{1}{2}\Omega_p\right) \int_{-\infty}^{\infty} d\nu \int_{-\infty}^{\infty} dz [Y(\nu_f - \nu, \nu, z) \right. \\
& \left. + Y(\nu, \nu_f - \nu, z)] \right|^2. \tag{B2}
\end{aligned}$$

The importance of the atomic response function being separated from the integral should be noted. Essentially this means that the spectral properties of the light may be considered apart from the structure of the absorber. The remaining integral is not difficult to perform,

$$\begin{aligned}
& \int_0^L dz \int_{-\infty}^{\infty} d\nu Y(\nu_f - \nu, \nu, z) \\
& = \frac{\pi}{U_2} e^{-\mathcal{D}\nu_p^2[(u_e + U_2)^2/\sigma_e^2 + u_e^2/\sigma_e^2 + \sigma_o^2 U_2^2 + 1/\sigma_p^2]} \\
& \quad \times [\text{erf}(\mathcal{E}\nu_p) - \text{erf}(\mathcal{E}\nu_p - \mathcal{L})],
\end{aligned}$$

where U_2 , u_e , \mathcal{E} , and \mathcal{L} are defined in the main text in Eq. (9). The integral over $Y(\nu, \nu_f - \nu, z)$ differs only by a constant factor.

However, the utility of this expression is limited. It only describes the probability of a single frequency from the pump beam being absorbed. Furthermore, it implies that this frequency will be on resonant with the final level. Realistically, all frequencies will have a chance to be absorbed and only $\nu_f=0$ will be resonant. To correct for this we can average the function over a Lorentzian line shape with its peak at $\nu_f=0$ and a height of 1. The full equation is given in the main text by Eq. (8).

APPENDIX C: THE FAIR COMPARISON COHERENT STATE

Again, our $|2::0\rangle$ state is produced from a photon pair from a type-II spontaneous parametric down-conversion event, incident on two filters and a symmetric beam splitter. We can examine $|\Psi\rangle$, Eq. (1), and see that—given the assumptions in Appendix A—this state has a spectral profile (the relative probability amplitude of the photons having frequencies ν_e and ν_o) given by

$$F_{|2::0\rangle}(\nu_e, \nu_o) = C \int_0^L dz e^{-\mathcal{D}(\nu_e + \nu_o)^2/\sigma_p^2} e^{iz((\nu_e + \nu_o)/U_p - \nu_e/U_e - \nu_o/U_o)}.$$

$|\Psi\rangle$ represents two entangled down-conversion modes. To remove the nonclassical nature of this light we project out one of the modes. We arbitrarily choose the ordinary mode. The remaining state will have the spectral profile we desire for one mode of our fair coherent state (F_α), that is,

$$\int_{-\infty}^{\infty} d\nu_o \langle 1_{\nu_o} | \Psi \rangle = \sqrt{\frac{\pi\sigma_p^2}{\mathcal{D}}} \sum_{k'} F_{\alpha, z}(\nu_e) \hat{a}_{ek'}^\dagger |0\rangle_e,$$

$$F_\alpha(\nu_e) = \int_0^L dz e^{-iz\nu_e(u_o-u_e)} e^{-u_o^2 z^2 \sigma_p^2 / 4D},$$

where $u_e = 1/U_p - 1/U_e$ and $u_o = 1/U_p - 1/U_o$. This will represent one mode of the ‘‘fair comparison’’ coherent light. The normalization will be discussed shortly. The other mode will have a separate, but identical, spectral profile. Both modes will be mixed with a symmetric beam splitter.

$$\begin{aligned} G_\alpha^{(2)}(t_1^d, t_2^d, t_1^d, t_2^d) &= \xi^4 \otimes_\nu \left\langle \frac{\alpha + i\beta}{\sqrt{2}} \gamma_3 \right|_{3\nu} \left\langle \frac{i\alpha + \beta}{\sqrt{2}} \gamma_4 \right|_{4\nu} \sum_{3\nu} \hat{a}_{3\nu}^\dagger e^{i(\nu_a + \Omega)t_1^d} e^{-D(\nu_d/\sigma')^2} \sum_{\nu_b} \hat{a}_{4\nu_b}^\dagger e^{i(\nu_b + \Omega)t_2^d} e^{-D(\nu_b/\sigma')^2} \\ &\times \sum_{\nu_c} \hat{a}_{3\nu_c} e^{-i(\nu_c + \Omega)t_1^d} e^{-D(\nu_c/\sigma')^2} \sum_{\nu_d} \hat{a}_{4\nu_d} e^{-i(\nu_d + \Omega)t_2^d} e^{-D(\nu_d/\sigma')^2} \otimes_\nu \left| \frac{\alpha + i\beta}{\sqrt{2}} \gamma_3 \right\rangle_{3\nu} \left| \frac{i\alpha + \beta}{\sqrt{2}} \gamma_4 \right\rangle_{4\nu} \\ &= \xi^4 \pi^2 |\gamma_3|^2 |\gamma_4|^2 e^{i\Omega(t_1^d + t_2^d - t_1^d - t_2^d)} \hat{\mathcal{F}}(\nu_a \rightarrow t_1^d) \hat{\mathcal{F}}(\nu_b \rightarrow t_2^d) \hat{\mathcal{F}}(\nu_c \rightarrow t_1^d) \hat{\mathcal{F}}(\nu_d \rightarrow t_2^d) [F_\alpha^*(\nu_a) - iF_\beta^*(\nu_a)] \\ &\times [-iF_\alpha^*(\nu_b) + F_\beta^*(\nu_b)] [F_\alpha(\nu_c) + iF_\beta(\nu_c)] [iF_\alpha(\nu_d) + F_\beta(\nu_d)], \end{aligned}$$

where the factors γ are the normalizations in the indexed modes. The central frequencies (Ω) have been taken to be the same. The filters in the arms $\sigma_e = \sigma_o$ have been removed in order to make the calculation which follows mathematically tractable. The frequencies have been labeled $a, b, c,$ and d . As before ξ represents the constants associated with the electric-field operators. We shall eventually take the two two-photon absorption probabilities in ratio, the ξ 's will cancel exactly. In light of this we simply set $\xi = 1$. We need to normalize such that the information about the intensity of the coherent light in each arm is contained in the γ 's,

$$\begin{aligned} I &= \int_{-\infty}^{\infty} dt \otimes_\omega \langle \gamma \alpha_\omega | \sum_{\omega'} \hat{a}_{\omega'}^\dagger e^{i\omega' t} \sum_{\omega''} \hat{a}_{\omega''} e^{-i\omega'' t} \otimes_\omega | \gamma \alpha_\omega \rangle \\ &= |\gamma|^2 \int_{-\infty}^{\infty} d\omega' \int_{-\infty}^{\infty} d\omega'' \delta(\omega' - \omega'') F_\alpha^*(\omega') F_\alpha(\omega'') \\ &= |\gamma|^2 \int_{-\infty}^{\infty} d\omega' |F_\alpha(\omega')|^2 \\ &= |\gamma|^2 \int_{-\infty}^{\infty} d\nu' \int_0^L dz_1 \int_0^L dz_2 e^{i(z_1 - z_2)\nu'} e^{-u_o^2 \sigma_p^2 (z_1^2 + z_2^2) / 4D} \\ &= \frac{|\gamma|^2 \sqrt{2\pi}}{u_o - u_e} \int_0^L dz_1 \int_0^L dz_2 \delta(z_1 - z_2) e^{-u_o^2 \sigma_p^2 (z_1^2 + z_2^2) / 4D}. \end{aligned}$$

The double integral is tractable yielding the result

$$\gamma = \left(\frac{I^2 (u_o - u_e)^2 u_o^2 \sigma_p^2}{D \pi^2} \right)^{1/4} \operatorname{erf} \left(\frac{L u_o \sigma_p}{\sqrt{2D}} \right)^{-1/2}.$$

Using the same procedure as in Eq. (B1) we obtain the spectral correlation function

In order to assimilate this spectral information into a coherent state we identify the spectral profile with α , thus, $\alpha_k = F_{\alpha_k}(\nu_k)$. The beam splitter transformation operating on the displacement operators which create the two-mode coherent state, $|\alpha\rangle_1 |\beta\rangle_2$, produces an output of $|\frac{\alpha+i\beta}{\sqrt{2}}\rangle_3 |\frac{i\alpha+\beta}{\sqrt{2}}\rangle_4$, where 1 and 2 label the input modes and 3 and 4 label the output modes.

So now we can write the temporal correlation function for the fair coherent state

$$\begin{aligned} S^{(2)} &= 2\pi^2 |\gamma_3|^2 |\gamma_4|^2 [F_\alpha^*(\nu_1') - iF_\beta^*(\nu_1')] [F_\alpha(\nu_1) + iF_\beta(\nu_1)] \\ &\times [iF_\alpha(\nu_2) + F_\beta(\nu_2)] [F_\beta^*(\nu_2') - iF_\alpha^*(\nu_2')]. \end{aligned}$$

Now we can write the two-photon absorption probability Eq. (2) as

$$\begin{aligned} P_2^\alpha &= \pi^2 |\gamma|^4 \left| \int_{-\infty}^{\infty} d\nu F_\alpha(\nu_f - \nu) F_\alpha(\nu) \right|^2 \\ &= \pi^2 |\gamma|^4 \left| \int_{-\infty}^{\infty} \frac{d\nu_u}{u_o - u_e} \int_0^L dz_1 \int_0^L dz_2 \right. \\ &\quad \times \left. e^{-iz_2 \nu_f (u_o - u_e)} e^{-i(z_1 - z_2)\nu_u} e^{-u_o^2 \sigma_p^2 (z_1^2 + z_2^2) / 4D} \right|^2 \\ &= \frac{\pi^2 |\gamma|^4}{(u_o - u_e)^2} \left| \int_0^L dz_1 \int_0^L dz_2 e^{-iz_2 \nu_f (u_o - u_e)} \right. \\ &\quad \times \left. \delta(z_1 - z_2) e^{-u_o^2 \sigma_p^2 (z_1^2 + z_2^2) / 4D} \right|^2 \\ &= \frac{\pi^3 D |\gamma|^4}{2u_o^2 \sigma_p^2 (u_o - u_e)^2} e^{-D(u_o - u_e)^2 \nu_f^2 / u_o^2 \sigma_p^2} \\ &\quad \times |\operatorname{erf}(\mathcal{E}_\alpha \nu_f) - \operatorname{erf}(\mathcal{E}_\alpha \nu_f + \mathcal{L}_\alpha)|^2, \end{aligned}$$

where \mathcal{E}_α and \mathcal{L}_α are defined in the main text. In the interest of simplicity the initial coherent states have been taken to be equivalent. As in Appendix B we must now take the integral of the above expression, times a Lorentzian line shape, over ν_f . This new function, \tilde{P}_2^α , is given in the main text by Eq. (11).

- [1] M. Tsang, Phys. Rev. A **75**, 043813 (2007).
- [2] A. N. Boto, P. Kok, D. S. Abrams, S. L. Braunstein, C. P. Williams, and J. P. Dowling, Phys. Rev. Lett. **85**, 2733 (2000).
- [3] R. W. Boyd and S. J. Bently, J. Mod. Opt. **53**, 713 (2006).
- [4] H. Lee, P. Kok, and J. P. Dowling, e-print arXiv:quant-ph/0306113.
- [5] V. Giovannetti, S. Lloyd, and L. Maccone, Phys. Rev. Lett. **96**, 010401 (2006).
- [6] J. Gea-Banacloche, Phys. Rev. Lett. **62**, 1603 (1989).
- [7] J. Javanainen and P. L. Gould, Phys. Rev. A **41**, 5088 (1990).
- [8] N. Ph. Georgiades, E. S. Polzik, K. Edamatsu, and H. J. Kimble, Phys. Rev. Lett. **75**, 3426 (1995).
- [9] G. S. Agarwal, Phys. Rev. A **1**, 1445 (1970).
- [10] I. V. Sokolov, Zh. Eksp. Teor. Fiz. **72**, 1687 (1977).
- [11] S. E. Harris, Phys. Rev. Lett. **98**, 063602 (2007).
- [12] S. Du, J. Wen, and C. Belthangady, Phys. Rev. A **79**, 043811 (2009).
- [13] D. V. Strekalov, M. C. Stowe, M. V. Chekhova, and J. P. Dowling, J. Mod. Opt. **49**, 2349 (2002).
- [14] B. Dayan, A. Pe'er, A. A. Friesem, and Y. Silberberg, Phys. Rev. Lett. **93**, 023005 (2004).
- [15] A. Joobeur, B. E. A. Saleh, T. S. Larchuk, and M. C. Teich, Phys. Rev. A **53**, 4360 (1996).
- [16] M. Hendrych, Xiaojuan Shi, A. Valencia, and Juan P. Torres, Phys. Rev. A **79**, 023817 (2009).
- [17] B. Dayan, Phys. Rev. A **76**, 043813 (2007).
- [18] Kevin A. O'Donnell and Alfred B. U'Ren, Phys. Rev. Lett. **103**, 123602 (2009).
- [19] Morton H. Rubin, David N. Klyshko, Y. H. Shih, and A. V. Sergienko, Phys. Rev. A **50**, 5122 (1994).
- [20] C. K. Hong, Z. Y. Ou, and L. Mandel, Phys. Rev. Lett. **59**, 2044 (1987).
- [21] D. S. Elliott, M. W. Hamilton, K. Arnett, and S. J. Smith, Phys. Rev. A **32**, 887 (1985).
- [22] Ce Chen, D. S. Elliott, and M. W. Hamilton, Phys. Rev. Lett. **68**, 3531 (1992).
- [23] B. R. Mollow, Phys. Rev. **175**, 1555 (1968).
- [24] R. J. Glauber, Phys. Rev. **130**, 2529 (1963).
- [25] T. E. Keller and M. H. Rubin, Phys. Rev. A **56**, 1534 (1997).
- [26] Y.-H. Kim, V. Berardi, M. V. Chekhova, A. Garuccio, and Y. Shih, Phys. Rev. A **62**, 043820 (2000).
- [27] Yoon-Ho Kim, Doctoral thesis dissertation, University of Maryland, 2001.
- [28] Y. Shih, Rep. Prog. Phys. **66**, 1009 (2003).
- [29] D. N. Nikogosyan, Appl. Phys. A: Mater. Sci. Process. **52**, 359 (1991).
- [30] C. Kurtsiefer, M. Oberparleiter, and H. Weinfurter, Phys. Rev. A **64**, 023802 (2001).
- [31] H.-B. Fei, B. M. Jost, S. Popescu, B. E. A. Saleh, and M. C. Teich, Phys. Rev. Lett. **78**, 1679 (1997).
- [32] M. R. Harpham, Ö. Süzer, C.-Q. Ma, P. Bäuerle, and T. Goodson III, J. Am. Chem. Soc. **131**, 973 (2009).
- [33] D.-I. Lee and T. Goodson III, J. Phys. Chem. B **110**, 25582 (2006).